



## FULL LENGTH ARTICLE

# Niclosamide (NA) overcomes cisplatin resistance in human ovarian cancer

Linjuan Huang<sup>a,b</sup>, Jing Zhang<sup>a,b</sup>, Youling Deng<sup>a,b</sup>,  
 Hao Wang<sup>b,c</sup>, Piao Zhao<sup>a,b</sup>, Guozhi Zhao<sup>a,b</sup>, Wei Zeng<sup>b,d</sup>,  
 Yonghui Wang<sup>b,e</sup>, Connie Chen<sup>b</sup>, William Wagstaff<sup>b</sup>,  
 Rex C. Haydon<sup>b</sup>, Russell R. Reid<sup>b,f</sup>, Tong-Chuan He<sup>b,g</sup>,  
 Le Shen<sup>b,g</sup>, Hue H. Luu<sup>b</sup>, Ling Zhao<sup>a,b,\*</sup>

<sup>a</sup> Departments of Obstetrics and Gynecology, Orthopaedic Surgery and Urology, The First Affiliated Hospital of Chongqing Medical University, Chongqing 400046, China

<sup>b</sup> Molecular Oncology Laboratory, Department of Orthopaedic Surgery and Rehabilitation Medicine, The University of Chicago Medical Center, Chicago, IL 60637, USA

<sup>c</sup> Ministry of Education Key Laboratory of Diagnostic Medicine, and Department of Clinical Biochemistry, The School of Laboratory Medicine, Chongqing Medical University, Chongqing 400016, China

<sup>d</sup> Department of Neurology, The Second Affiliated Hospital of Jiangnan University, Wuhan, Hubei 430050, China

<sup>e</sup> Department of Clinical Laboratory Medicine, Shanghai Jiaotong University School of Medicine, Shanghai 200000, China

<sup>f</sup> Laboratory of Craniofacial Suture Biology and Development, Department of Surgery Section of Plastic Surgery, The University of Chicago Medical Center, Chicago, IL 60637, USA

<sup>g</sup> Department of Surgery, The University of Chicago Medical Center, Chicago, IL 60637, USA

Received 21 August 2022; received in revised form 8 November 2022; accepted 4 December 2022

Available online 2 January 2023

## KEYWORDS

Chemotherapy  
 resistance;  
 Cisplatin;  
 Drug repurposing;  
 Niclosamide;  
 Ovarian cancer

**Abstract** Ovarian cancer (OC) is one of the most lethal malignancies of the female reproductive system. OC patients are usually diagnosed at advanced stages due to the lack of early diagnosis. The standard treatment for OC includes a combination of debulking surgery and platinum-taxane chemotherapy, while several targeted therapies have recently been approved for maintenance treatment. The vast majority of OC patients relapse with chemoresistant tumors after an initial response. Thus, there is an unmet clinical need to develop new therapeutic agents to overcome the chemoresistance of OC. The anti-parasite agent niclosamide (NA) has been repurposed as an anti-cancer agent and exerts potent anti-cancer activities in human cancers including OC. Here, we investigated whether NA could be repurposed as a therapeutic

\* Corresponding author. Department of Obstetrics and Gynecology, The First Affiliated Hospital, Chongqing Medical University, Chongqing 400046, China

E-mail address: [zl203047@hospital-cqmu.com](mailto:zl203047@hospital-cqmu.com) (L. Zhao).

Peer review under responsibility of Chongqing Medical University.

agent to overcome cisplatin-resistant (CR) in human OC cells. To this end, we first established two CR lines SKOV3CR and OVCAR8CR that exhibit the essential biological characteristics of cisplatin resistance in human cancer. We showed that NA inhibited cell proliferation, suppressed cell migration, and induced cell apoptosis in both CR lines at a low micromole range. Mechanistically, NA inhibited multiple cancer-related pathways including AP1, ELK/SRF, HIF1, and TCF/LEF, in SKOV3CR and OVCAR8CR cells. NA was further shown to effectively inhibit xenograft tumor growth of SKOV3CR cells. Collectively, our findings strongly suggest that NA may be repurposed as an efficacious agent to combat cisplatin resistance in chemoresistant human OC, and further clinical trials are highly warranted.

© 2023 The Authors. Publishing services by Elsevier B.V. on behalf of KeAi Communications Co., Ltd. This is an open access article under the CC BY-NC-ND license (<http://creativecommons.org/licenses/by-nc-nd/4.0/>).

## Introduction

Ovarian cancer is the third most common malignant tumor of the female reproductive system and the second most common cause of gynecologic cancer death in women around the world.<sup>1–3</sup> Due to the lack of early screening and diagnosis techniques, most ovarian cancer patients are diagnosed at an advanced stage, leading to poor outcomes for this disease. Therefore, the five-year survival rates remain below 50%.<sup>1,3</sup> Approximately 90% of ovarian cancers are epithelial, and the four most common histological types of epithelial ovarian cancer (EOC) are serous, endometrioid, clear cell, and mucinous, some of which can be further classified into more subtypes based on their specific biology and treatment responses.<sup>1–3</sup> It has been estimated that a female individual's lifetime risk to develop ovarian cancer is 1 in 75, and their chance to die of this disease is 1 in 100.<sup>4</sup> While the cellular origin and pathogenesis of ovarian cancer remain to be fully understood, several risk factors and numerous genetic susceptibilities have been reported.<sup>2–4</sup> Some of the reported risk factors include hormonal and reproductive factors such as incessant ovulation and gonadotropin exposure, early age at menarche and late age at menopause, parity and infertility, lack of lactation, benign gynecologic conditions such as polycystic ovarian syndrome and endometriosis, and hormone replacement therapy. However, one of the most significant risk factors for ovarian cancer is a positive family history of breast or ovarian cancer.<sup>4</sup> High penetrant mutations in the *BRCA1* and *BRCA2* genes greatly increase lifetime risk and account for the majority of hereditary cases and 10%–15% of all cases.<sup>4,5</sup> Other familial syndromes such as hereditary non-polyposis colorectal cancer syndrome (HNPCC), and mutations in DNA repair genes, are significant risk factors.<sup>4</sup> The known syndromes account for 36% of ovarian cancer familial relative risk, while genome-wide association studies have identified 22 susceptibility alleles for invasive ovarian cancer with weak to moderate effects.<sup>4,6</sup>

The standard ovarian cancer treatment includes debulking surgery and/or platinum-taxane chemotherapy.<sup>3,7</sup> Neoadjuvant chemotherapy is used to decompress the tumor burden for poor surgical candidates with a low likelihood of

optimal cytoreduction, whereas patients with a favorable surgical profile receive either neoadjuvant chemotherapy or undergo cytoreduction surgery.<sup>3,7,8</sup> For the past several years, a series of novel small molecule inhibitors and humanized monoclonal antibodies, such as anti-angiogenic inhibitors pazopanib and bevacizumab, and poly(ADP-ribose) polymerase (PARP) inhibitors olaparib, veliparib, and niraparib, have been used for maintenance therapy, some of which have significantly improved progression-free survival.<sup>3,7,8</sup> While ovarian cancer is one of the most chemoresponsive tumors, patients will relapse with chemoresistant tumors after an initial response and about 80% of patients with advanced-stage ovarian cancer experience cancer recurrence.<sup>7,8</sup> Thus, there is an unmet clinical need to identify new and effective therapeutic agents to overcome platinum resistance in ovarian cancer.

Repurposing drugs represent a cost-effective and time-saving strategy to identify new therapeutic applications for the approved drugs or investigational drugs that are outside the scope of the originally approved indications.<sup>9,10</sup> Drug repurposing is particularly popular in the cancer drug discovery community, and several repurposed drugs have entered various phases of clinical trials.<sup>11–13</sup> Niclosamide (NA) represents one of the most promising repurposing drug candidates for cancer.<sup>14</sup> Niclosamide is a drug approved by the US Food and Drug Administration (FDA) to treat tapeworm infection since the 1960s.<sup>11–14</sup> It has been reported that NA exerts strong anti-cancer activities in several types of human cancers.<sup>14–31</sup> We previously demonstrated that blockade of IGF signaling sensitized human ovarian cancer cells to niclosamide-induced anti-proliferative and anti-cancer activities.<sup>32</sup> Nonetheless, it is unclear whether NA exerts strong cytotoxicity in cisplatin-resistant (CR) ovarian cancer.

In this study, we sought to investigate whether NA could be repurposed as an effective therapeutic agent to overcome cisplatin resistance in human ovarian cancer cells. Here, we first established two robust CR human ovarian cancer lines OVCAR8CR and SKOV3CR and demonstrated both CR lines exhibited the essential biological characteristics of cisplatin resistance in human cancer. NA was shown to effectively inhibit cell proliferation, suppress cell migration, and induce cell apoptosis in the CR ovarian

cancer cells at a very low micromole range. We further demonstrated NA effectively inhibited xenograft tumor growth of the SKOV3CR cells. Mechanistically, NA was shown to inhibit multiple cancer-related pathways, especially AP1, ELK/SRF, HIF1, and TCF/LEF, in the CR ovarian cancer cells. Collectively, our findings suggest that NA may be repurposed as a novel efficacious agent to overcome cisplatin resistance in chemoresistant human ovarian cancer.

## Materials and methods

### Cell culture and chemicals

Human epithelial ovarian cancer cell lines OVCAR8 and SKOV3, as well as the high-grade serous ovarian cancer (HGSOC) cell lines OVPA8 and OVCAR3, were generously provided by Dr. Ernest Lengyel of The University of Chicago. All cells were maintained in complete Dulbecco's Modified Eagle's Medium (DMEM) supplemented with 10% fetal bovine serum (FBS, Gemini Bio-Products, West Sacramento, CA, USA), 100 units of penicillin and 100  $\mu$ g of streptomycin at 37 °C in 5% CO<sub>2</sub> as described.<sup>33–35</sup> Niclosamide (NA) was purchased from Sigma–Aldrich (St. Louis, MO, USA), and cisplatin was purchased from Selleckchem (Houston, TX, USA). Unless otherwise indicated, other chemicals were purchased from either Thermo-Fisher Scientific (Waltham, MA, USA) or Sigma–Aldrich.

### Development of cisplatin-resistant (CR) human epithelial ovarian cancer cell lines OVCAR8CR and SKOV3CR

Exponentially growing OVCAR8 and SKOV3 cells were initially treated with 0.05  $\mu$ M cisplatin (dissolved in dimethylformamide or DMF; the cisplatin stock solution was aliquoted and kept at –80 °C) for 72 h. The viable cells were replated and grew, followed by dose-escalating selections of cisplatin concentrations gradually to 10  $\mu$ M, yielding the stable cisplatin-resistant (CR) lines, designated as OVCAR8CR and SKOV3CR.<sup>36</sup> These CR cell lines were further characterized in this study.

### Crystal violet viability staining

Crystal violet staining assay was conducted as described.<sup>37–39</sup> Briefly, subconfluent OVCAR8CR, SKOV3CR, and/or their parental lines were treated with various concentrations of cisplatin or niclosamide for 72 h. The cells were washed with PBS and stained with crystal violet/formalin mix at room temperature for 20 min. The stained cells were washed with tap water gently, air dried, and scanned for macrographic images. For quantitative analysis, the stained cells were dissolved with 30% acetic acid and measured for absorbance at 570–590 nm. Each conditioned assay was carried out in triplicate. Relative optical density (OD) was calculated by dividing the average OD values of the drug treatment groups

by that of the respective control group treated with 0  $\mu$ M drug (*i.e.*, vehicle control).

### WST-1 cell proliferation assay

Cell proliferation was assessed with premixed WST-1 reagent (Takara Bio USA Inc., Mountain View, CA, USA) as described.<sup>40–43</sup> Briefly, cells were seeded into 96-well culture plates and treated with varying concentrations of cisplatin or niclosamide for 72 h. The freshly prepared WST-1 Working Mix was added into each well and incubated at 37 °C for 2 h before subjecting plate reading at 450 nm using a microplate reader. IC50 values were calculated by using Graph Pad Prism 8.4.0. Each conditioned assay was done in triplicate.

### Wound healing/cell migration assay

Wound healing/cell migration assay was performed as described.<sup>44–46</sup> Experimentally, cells were seeded in 6-well plates and grew to 90% confluence. The monolayer cells were then scratched with sterile micro-pipette tips, and treated with different concentrations of NA. The wound closure status at the same locations was recorded under a bright field microscope at the indicated time points. Each assay was done in triplicate.

### Hoechst 33258 staining for apoptosis analysis

Hoechst 33258 staining assay was conducted as described.<sup>36,41,47,48</sup> Briefly, exponentially growing cells were treated with varying concentrations of niclosamide or cisplatin for 72 h. The treated cells were harvested, fixed, and stained with the Hoechst 33258. Apoptotic cells were analyzed under a fluorescence microscope. Each conditioned assay was done in triplicate.

### Total RNA isolation and touchdown-quantitative real-time PCR (TqPCR) analysis

Subconfluent parental human epithelial ovarian cancer lines OVCAR8 and SKOV3 and cisplatin-resistance human epithelial ovarian cancer cell lines OVCAR8CR and SKOV3CR were treated with various conditions for 48 h. Total RNA was isolated from treated cells by using the NucleoZOL reagent (Takara Bio USA Inc) and subjected to reverse transcription (RT) reactions with hexamer, M-MuLV reverse transcriptase (New England Biolabs, Ipswich, MA), and dNTPs (GenScript USA Inc. Piscataway, NJ, USA). RT products were used as qPCR templates. The qPCR primers for the genes of interest were designed by using the Primer3 Plus program (Table S1). TqPCR reactions were carried out by using SYBR Green-based Forget-Me-Not™ qPCR Master Mix (Biotium Inc., Hayward, CA, USA) on a CFX-Connect unit (Bio-Rad Laboratories, Hercules, CA, USA) as described.<sup>42,49–53</sup> *GAPDH* was used as a reference gene. Relative expression was calculated by using the 2<sup>– $\Delta\Delta$ Ct</sup> method. All qPCR reactions were done in triplicate.

## Reporter plasmid DNA transfection and Gaussia luciferase assay

The transfection of the 12 cancer-associated pathway reporters and the Gaussia luciferase assay were performed as previously described.<sup>40,54,55</sup> These cancer-associated pathways included NFAT, HIF-1, TCF/LEF, E2F/DP1, ELK1/SRF, AP1, NF $\kappa$ B, SMAD, STAT1/2, RBP-JK, CREB, MYC/MAX pathway reporters. Briefly, exponentially growing SKOV3CR cells were seeded in 60-mm cell culture dishes and transfected with 5  $\mu$ g reporter plasmid DNA per dish of each reporter plasmid by using the PEI transfection reagent (Polysciences, Warrington, PA) as described.<sup>56–58</sup> At 18 h post-transfection, the transfected cells were replated into 24-well cell culture plates and treated with niclosamide at various concentrations or DMSO. At 24 h and/or 48 h after treatment, culture media were taken for Gaussia luciferase assays using the Gaussia Luciferase Assay Kit (GeneCopoeia, Rockville, MD) as previously described.<sup>59–62</sup> Each conditioned assay was done in triplicate.

## Treatment of the xenograft tumors of cisplatin-resistance human epithelial ovarian cancer cells

The use and care of animals for the reported work were approved by the Institutional Animal Care and Use Committee (IACUC) of The University of Chicago. The xenograft tumor model of human cisplatin-resistant ovarian cancer cells was established as previously described.<sup>63,64</sup> Specifically, exponentially growing firefly luciferase-tagged SKOV3CR cells were collected, resuspended in sterile PBS at the concentration of  $5 \times 10^7$  cells/mL, and injected subcutaneously into the flanks of athymic nude mice (Harlan Laboratories; 5–6 weeks old, female;  $5 \times 10^6$  cells per injection; 6 injection sites and 3 injections on each side per mouse).

For the NA treatment, at 7 days post-implantation, the mice were randomized and divided into three groups ( $n = 6$  per group), low dose niclosamide group (intraperitoneal injection of 10 mg/kg body weight, once every two days), high dose niclosamide group (intraperitoneal injection of 20 mg/kg body weight, once every two days), and DMSO control group (*i.e.*, 0 mg/kg body weight). Tumor growth was monitored by using the Xenogen IVIS 200 whole-body bioluminescence imaging system weekly. The average signals were calculated using Xenogen's Living Image analysis software as previously described.<sup>65–68</sup>

## Hematoxylin and eosin (H&E) staining & immunohistochemical (IHC) analysis

H&E histologic evaluation was performed as previously described.<sup>69–73</sup> Experimentally, the retrieved tumor masses were fixed with 10% PBS-buffered formalin and paraffin-embedded. Serial sections were deparaffinized and stained with hematoxylin and eosin. Staining results were photographed under a bright field microscope.

IHC analysis was conducted as previously described.<sup>74–77</sup> Briefly, the tissue sections were deparaffinized, rehydrated, and subjected to IHC staining with a PCNA antibody

(Santa Cruz Biotechnology, Dallas, TX, USA). Minus primary antibody and control IgG were used as negative controls.

## Statistical analysis

All quantitative experiments were done in triplicate and/or in three independent batches. Quantitative data were expressed as mean  $\pm$  standard deviation (SD). Statistical analysis was determined by one-way analysis of variance and the student's *t*-test. A *P*-value  $<0.05$  was defined as statistically significant.

## Results and discussion

### OVCAR8CR and SKOV3CR are stable cisplatin-resistant (CR) ovarian cancer cell lines

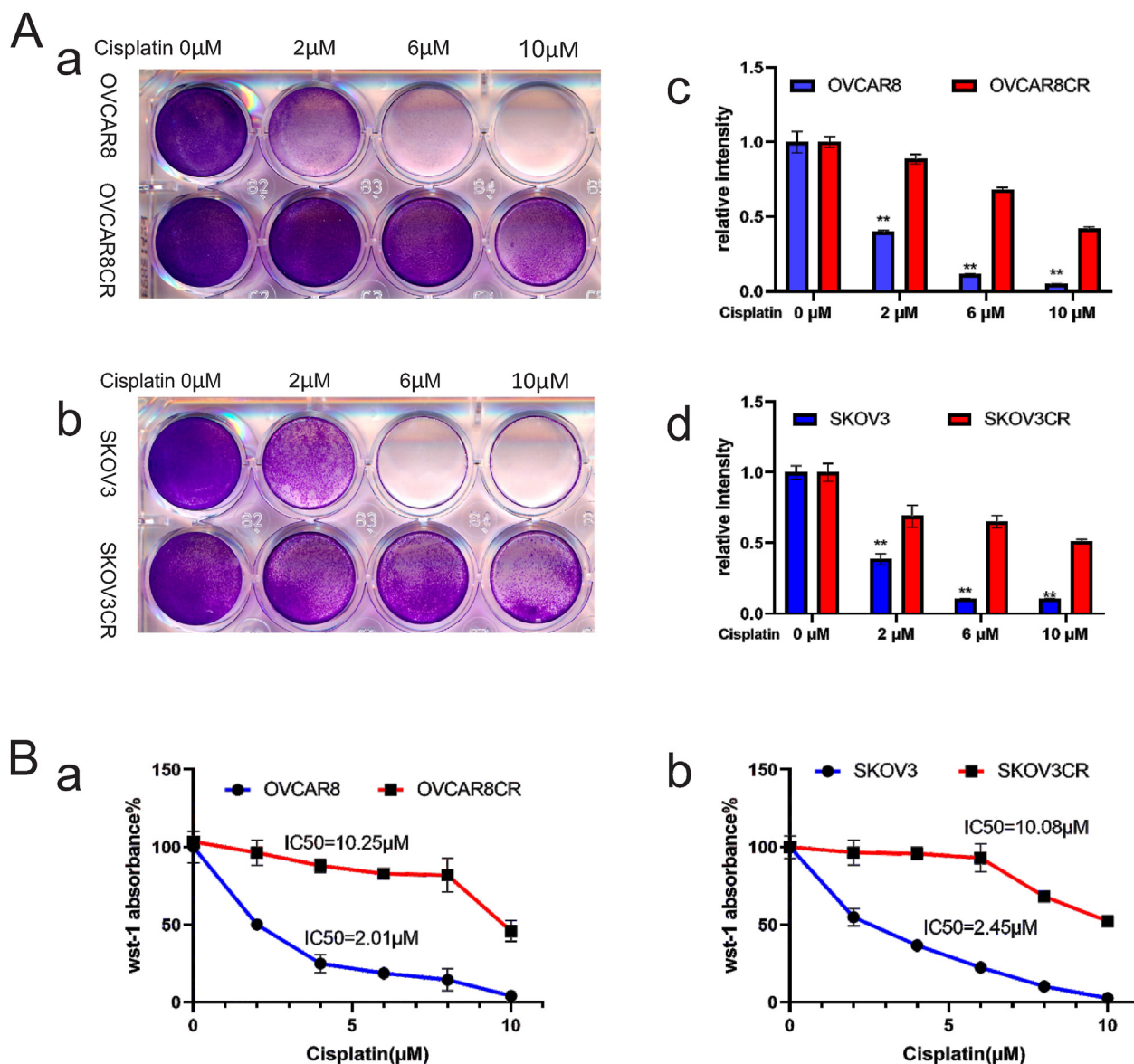
In order to establish stable cisplatin-resistant human ovarian cancer cell lines, we used two widely used OVCAR8 and SKOV3 cell lines and selected them for cell proliferation based on a dose-escalating selection scheme. Briefly, exponentially growing OVCAR8 and SKOV3 cells were initially treated with 0.05  $\mu$ M cisplatin, a relatively low sublethal concentration. Most cells were killed by cisplatin. The remaining surviving cells were replated, expanded, and then subjected to another round of selection of 0.05  $\mu$ M cisplatin, resulting in more surviving cells. Such selection cycles were repeated with escalating concentrations of cisplatin until the reach of stable resistance to 10  $\mu$ M cisplatin, which was designated as OVCAR8CR and SKOV3CR. The dose-escalating selection scheme took up to three months.

As shown by the crystal violet staining analysis, both OVCAR8CR and SKOV3CR survived 10  $\mu$ M cisplatin, while the parental cell lines OVCAR8 and SKOV3 were all killed at 6  $\mu$ M cisplatin (Fig. 1A, panels *a* & *b*). Quantitative analysis revealed that OVCAR8CR and SKOV3CR lines had significantly higher percentages of surviving cells than that of their parental counterparts (Fig. 1A, panels *c* & *d*).

We further examined the effect of cisplatin on cell proliferation of OVCAR8CR and SKOV3CR lines, in comparison with their respective parental lines OVCAR8 and SKOV3. We found that cisplatin inhibited cell proliferation of OVCAR8 cells in a dose-dependent fashion with IC<sub>50</sub> at 2.01  $\mu$ M, while the IC<sub>50</sub> value for OVCAR8CR cells was 10.25  $\mu$ M (Fig. 1B, panel *a*). Similarly, cisplatin effectively inhibited cell proliferation of SKOV3 in a dose-dependent fashion with IC<sub>50</sub> at 2.45  $\mu$ M, while the IC<sub>50</sub> for SKOV3CR was at 10.08  $\mu$ M (Fig. 1B, panel *b*).

### OVCAR8CR and SKOV3CR cells are apoptosis-resistant and express cisplatin resistance-associated genes upon cisplatin treatment

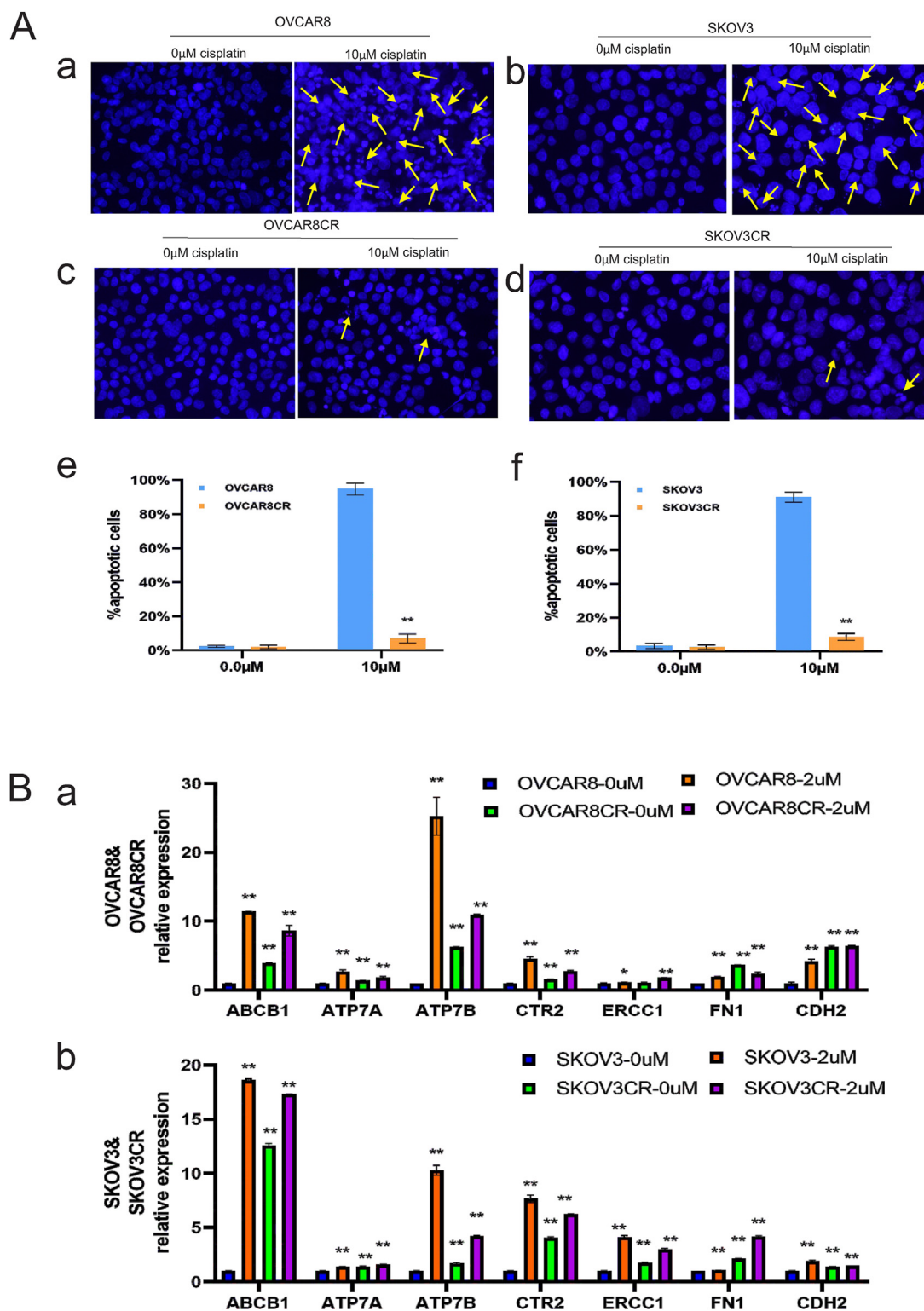
We next characterized the cisplatin-resistance features of these two lines. By comparing with their respective parental lines OVCAR8 and SKOV3, we showed that both OVCAR8CR and SKOV3CR cells were resistant to cisplatin-induced apoptosis (Fig. 2A, panels *a* vs. *b* and *c* vs. *d*). Quantitative analysis revealed that the % apoptotic cells



**Figure 1** Cell viability and proliferation capability of the cisplatin-resistant (CR) human ovarian cancer cell lines. (A) Cell viability assay. Subconfluent OVCAR8CR (a) and SKOV3CR (b) and parental lines OVCAR8 (a) and SKOV3 (b) were treated with varying concentrations of cisplatin for 72 h, followed by crystal violet staining. The stained cells were dissolved with 30% acetic acid and measured for absorbance at 570–590 nm. Each conditioned assay was carried out in triplicate. Relative optical density (OD) was calculated by dividing the average OD values of the cisplatin treatment groups by that of the respective control group treated with 0  $\mu$ M cisplatin (*i.e.*, DMF only) (c, d). **\*\*** $P < 0.01$ , compared with that of the CR lines. (B) WST-1 proliferation assay. Subconfluent OVCAR8CR (a) and SKOV3CR (b) cells were seeded in 96-well cell culture plates, treated with the indicated concentrations of cisplatin for 72 h, and incubated with the WST-1 reagent for an additional 2 h, followed by absorbance reading. IC<sub>50</sub> values were determined by using Graph Pad Prism 8.4.0. All conditioned assays were done in triplicate.

was significantly lower in OVCAR8CR (Fig. 2A, panel e) and SKOV3CR (Fig. 2A, panel f) cells than that in the respective parental lines ( $P < 0.01$ ). Thus, these results indicate that OVCAR8CR and SKOV3CR cells can survive and proliferate in the presence of cisplatin concentrations that are toxic to their parental lines. Even though the exact mechanism underlying cisplatin resistance remains to be fully understood, numerous studies have identified differential expression of many genes that were associated with cisplatin resistance.<sup>78–81</sup> We analyzed a panel of seven

genes that are associated with cisplatin resistance, and we found that, except *ERCC1*, the expression of *ABCB1*, *ATP7A*, *ATP7B*, *CTR2*, *FN1*, and *CDH2* was significantly up-regulated in the OVCAR8CR cells, compared with that in the parental OVCAR8 cells, and even all seven genes were up-regulated in OVCAR8 cells upon cisplatin treatment (Fig. 2B, panel a). Accordingly, we found the expression of these seven genes was significantly up-regulated in the SKOV3CR cells, compared with that of the SKOV3 cells, and all seven genes were up-regulated in SKOV3 cells upon cisplatin treatment



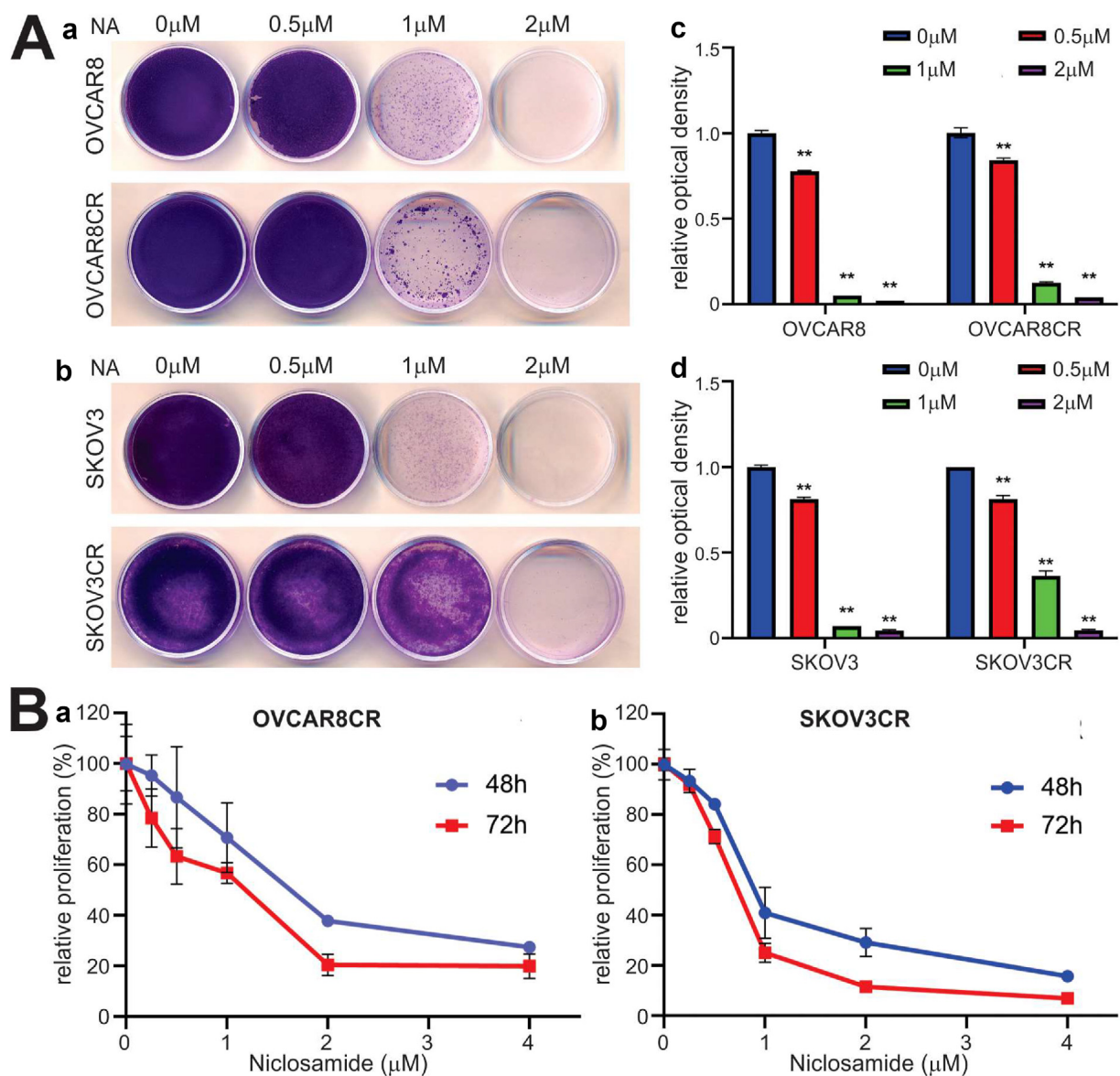


**Figure 3** Inhibitory effects of niclosamide (NA) on the cell viability and proliferation of human CR ovarian cancer lines. **(A)** Cell viability assay. Subconfluent OVCAR8 & OVCAR8CR **(a)** and SKOV3 & SKOV3CR **(b)** were treated with varying concentrations of NA for 72 h. The treated cells were fixed and subjected to crystal violet staining. The stained cells were dissolved with 30% acetic acid and measured for absorbance at 570–590 nm. Each conditioned assay was carried out in triplicate. Relative optical density (OD) was calculated by dividing the average OD values of the NA treatment groups by that of the respective control group treated with 0  $\mu$ M NA (*i.e.*, DMSO only) **(c, d)**. **\*\*** $P < 0.01$ , compared with that of the respective cells treated with 0  $\mu$ M NA (*i.e.*, DMSO control). **(B)** WST-1 cell proliferation assay. Subconfluent OVCAR8CR **(a)** and SKOV3CR **(b)** cells were seeded in 96-well cell culture plates and treated with varying concentrations of NA for 48 h and 72 h, followed by the addition of WST-1 reagent for additional 2-h incubation prior to the absorbance reading. All conditioned assays were done in triplicate.

(Fig. 2B, panel b). Collectively, these results demonstrate that the OVCAR8CR and SKOV3CR cell lines exhibit some of the essential biological characteristics of cisplatin resistance in human cancer.

#### Niclosamide (NA) inhibits the cell proliferation of OVCAR8CR and SKOV3CR cells

In order to search for potential therapeutic agents that can overcome cisplatin resistance, we assessed the anti-proliferative activity of niclosamide (NA) in these two cisplatin-

resistant lines. When both OVCAR8CR and parental OVCAR8 cells were treated with different concentrations of NA, we found that the numbers of viable cells drastically decreased at as low as 1.0  $\mu$ M of NA, and completely eliminated at 2.0  $\mu$ M of NA (Fig. 3A, panel a). The quantitative analysis further confirmed that NA significantly decreased the cell viability of both OVCAR8CR and OVCAR8 cells at as low as 1.0  $\mu$ M (Fig. 3A, panel b). Similar results were obtained in SKOV3CR and SKOV3 cells as we found that NA markedly decreased the cell viability of both SKOV3CR and SKOV3 cells at as low as 1.0  $\mu$ M although more cells survived in the

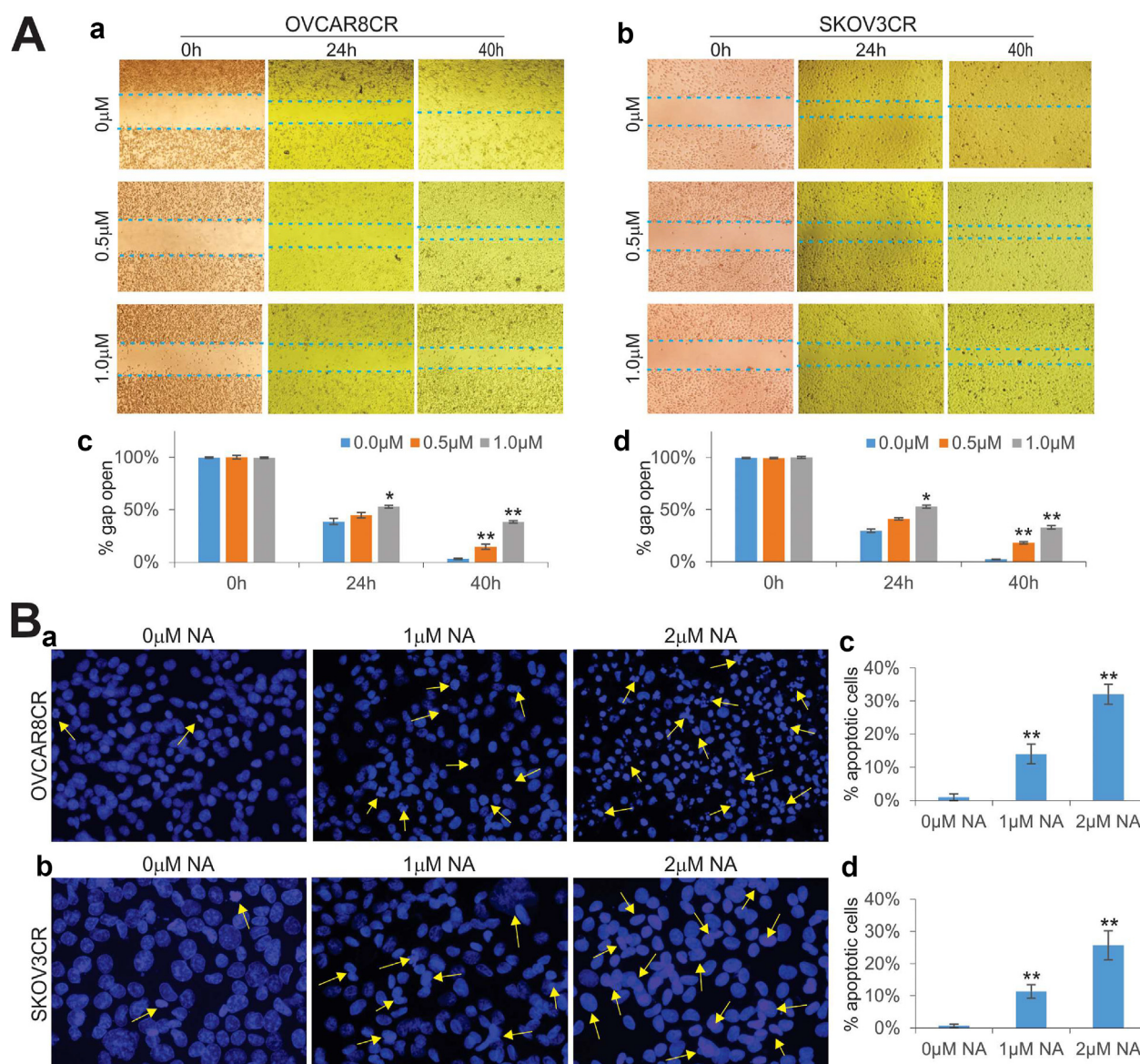


**Figure 4** NA inhibits wound healing/cell migration and induces apoptosis in the cisplatin resistance human ovarian cancer cells. **(A)** Wound healing/cell migration assay. Subconfluent OVCAR8CR **(a)** and SKOV3CR **(b)** cells were wounded with micro-pipette tips and treated with 0, 0.5, and 1.0  $\mu\text{M}$  NA. The wound gaps were recorded at 0, 24, and 40 h post-treatment. Representative results are shown. The wound gaps were quantitatively measured, and % gap opening was calculated for OVCAR8CR **(c)** and SKOV3CR **(d)** by using the gap distance at 0 h as 100% for each treatment group. \* $P < 0.05$ , \*\* $P < 0.01$ , compared with that of the cells treated with 0  $\mu\text{M}$  NA at respective time points. **(B)** Apoptosis assay. Subconfluent OVCAR8CR **(a)** and SKOV3CR **(b)** cells were treated with varying concentrations of NA for 72 h. The cells were harvested, fixed, and stained with Hoechst 33258. Representative apoptotic cells are indicated by arrows. Apoptotic cells were also counted and averaged in 10 random high-power fields (HPFs) for the calculation of % apoptotic cells for OVCAR8CR **(c)** and SKOV3CR **(d)**. \*\* $P < 0.01$ , compared with that of the cells treated with 0  $\mu\text{M}$  NA.

SKOV3CR cells (Fig. 3B, panel a). Quantitative analysis showed that NA significantly inhibited cell proliferation of SKOV3CR and SKOV3 cells in a dose-dependent fashion, and no viable cells were observed at 2.0  $\mu\text{M}$  of NA treatment (Fig. 3B, panel b). It is noteworthy that, while we only established cisplatin-resistant lines from low-grade epithelial ovarian cancer lines OVCAR8CR and OVCAR8, two commonly used high-grade serous ovarian cancer (HGSOC) cell lines OVPA8 and OVCAR3 were shown highly sensitive to NA treatment (Fig. S1A) and were nearly completely killed at 2.0  $\mu\text{M}$  NA (Fig. S1B), which is similar to the lethal

concentrations for OVCAR8CR and SKOV3CR lines, suggesting that NA may exert its potent anti-cancer activity independent of genetic and/or epigenetic alterations acquired in ovarian cancer development and/or chemoresistance.

We further examined the effect of NA on the cell proliferative activity of OVCAR8CR and SKOV3CR. Using the WST-1 assay, we demonstrated that NA inhibited OVCAR8CR cell proliferation in a dose-dependent fashion. Specifically, at the 1.0  $\mu\text{M}$  of NA, the viable cells decreased to 70.7% and 56.7% of the control group at 48 and 72 h, respectively. The viable OVCAR8CR cells at 2.0  $\mu\text{M}$  of NA further decreased to

37.8% and 20.5% of the control group at 48 and 72 h, respectively (Fig. 3B, panel a). Similarly, when SKOV3CR cells were treated with 1.0  $\mu\text{M}$  of NA, the viable cells decreased to 50.0% and 25.0% of the control group at 48 and 72 h, respectively; and at 2.0  $\mu\text{M}$  of NA, the viable cells further decreased to 29.1% and 11.6% of the control group at 48 h and 72 h, respectively (Fig. 3B, panel b). Collectively, these results suggest that NA may be able to inhibit cell viability and proliferative activity of the CR human ovarian cancer cells.

### NA inhibits wound healing/cell migration and induces apoptosis in cisplatin-resistant human ovarian cancer cells

We further investigated if NA inhibited wound healing/cell migration in cisplatin-resistance human ovarian cancer cells. NA was shown to inhibit wound healing/cell migration in OVCAR8CR cells in a dose- and time-dependent manner (Fig. 4A, panel a). Specifically, the OVCAR8CR cells failed to close the gap at 40 h when treated with 1.0  $\mu\text{M}$  of NA, while the DMSO control group was completely healed at the same time. Similar results were obtained in SKOV3CR cells as wound healing/cell migration was effectively inhibited by 1.0  $\mu\text{M}$  NA (Fig. 4A, panel b). Quantitative analysis revealed that cell wound closure was significantly inhibited in OVCAR8CR (Fig. 4A, panel c) and SKOV3CR (Fig. 4A, panel d) cells by 0.5  $\mu\text{M}$  NA at 40 h and 1.0  $\mu\text{M}$  NA at both 24 h and 40 h. These results demonstrated that NA inhibits cisplatin-resistance human ovarian cancer cell proliferation and migration at low micromole concentrations.

We also tested the effect of NA on cell apoptosis in cisplatin-resistance ovarian cancer cells. We found that, when OVCAR8CR and SKOV3CR cells were treated with 1.0  $\mu\text{M}$  and 2.0  $\mu\text{M}$  NA for 72 h, apoptotic cells were more readily observed in both cell lines, compared with that of the DMSO control group in a dose-dependent fashion (Fig. 4B, panels a & b), suggesting that NA may effectively induce cell apoptosis in cisplatin-resistance human ovarian cancer cells.

Collectively, these results strongly suggest that human cisplatin-resistance ovarian cancer cells are sensitive to NA treatment. NA can reduce cell viability, inhibit cell proliferation and wound healing/cell migration, and induce cell apoptosis.

### NA inhibits multiple cancer-associated signal pathways in cisplatin-resistance human ovarian cancer cells

Mechanistically, it has been reported that NA may exert anti-cancer activity by inhibiting multiple cellular signal pathways.<sup>14–32</sup> Here, we sought to determine whether NA would overcome cisplatin-based chemoresistance in human ovarian cancer cells through similar mechanisms. By using a panel of *Gaussia luciferase* (GLuc) reporters for 12 cancer-related signal pathways,<sup>40,54</sup> we tested the effect of NA on the 12 cancer-related signal pathways in the cisplatin-resistant human ovarian cancer cells. When the GLuc reporters were transfected into SKOV3CR cells and then treated with various concentrations of NA for 48 h, we

found that 11 of the 12 cancer-related pathway reporters were significantly inhibited by NA in a dose-dependent fashion (Fig. 5A). Interestingly, the CREB-GLuc reporter was activated at 4  $\mu\text{M}$  of NA after 48 h. Nonetheless, the results suggest that NA may suppress cisplatin chemoresistance in ovarian cancer cells by inhibiting multiple cancer-related signal pathways.

We further analyzed the inhibitory effect of NA on the four most affected pathways, AP1, ELK/SRF, HIF1, and TCF/LEF in SKOV3CR cells. We found that AP1 reporter activities were significantly inhibited by NA at 24 h and 48 h in a dose-dependent or time-dependent fashion (Fig. 5B, panel a). Similar results were obtained for the ELK/SRF pathway (Fig. 5B, panel b), the HIF1 pathway (Fig. 5B, panel c), and the TCF/LEF pathway (Fig. 5B, panel d). Furthermore, we demonstrated that the AP1, ELK/SRF, HIF1, and TCF/LEF pathways were also effectively inhibited by NA in OVCAR8CR cells in both time- and dose-dependent fashions (Fig. S2, panels a–d). Collectively, these results strongly suggest that NA may primarily target cell proliferation and cell survival pathways in overcoming cisplatin resistance in human ovarian cancer cells.

### NA suppress tumor growth in the xenograft model of cisplatin-resistance human ovarian cancer cells

Lastly, we analyzed the effect of NA on *in vivo* tumor growth of cisplatin-resistant ovarian cancer cells. To establish the xenograft tumor model, we stably tagged the OVCAR8CR cells with firefly luciferase and injected the cells into the flanks of athymic nude mice. At three days post-injection, the mice were divided into two doses of NA-treated groups (10 mg/kg body weight and 20 mg/kg body weight) and the vehicle control group. Tumor growth was monitored by using Xenogen bioluminescence imaging for up to 24 days post-treatment, which showed remarkable decreases in imaging signals in the treatment groups (Fig. 6A, panel a). Further quantitative analysis revealed that NA effectively inhibited tumor growth at 17 and 24 days after NA treatment, compared with that of the vehicle control group (Fig. 6A, panel b). At the endpoint, the tumor masses were retrieved, and the vehicle control group had larger average tumor masses individually (Fig. 6B, panel a) and the largest bulk volume of retrieved tumors (Fig. 6B, panel b).

H&E histologic analysis of the retrieved tumor masses revealed that xenograft tumors treated with NA exhibited significant necrosis and decreased cellularity, compared with that of the control group (Fig. 6C, panel a). Immunohistochemical staining analysis of the cell proliferative marker PCNA indicated that the cell proliferation was effectively inhibited in the xenograft tumors treated with NA, especially in the high NA dose group (20 mg/kg body weight) (Fig. 6C, panel b). NA-induced apoptosis was also confirmed by immunohistochemical staining analysis with cleaved Caspase-3 antibody (Fig. S3). Collectively, these *in vivo* findings showed that NA effectively suppressed the xenograft tumor growth of cisplatin-resistance human ovarian cancer cells, suggesting that NA may be used as an efficacious therapeutic agent to overcome cisplatin resistance in ovarian cancer.

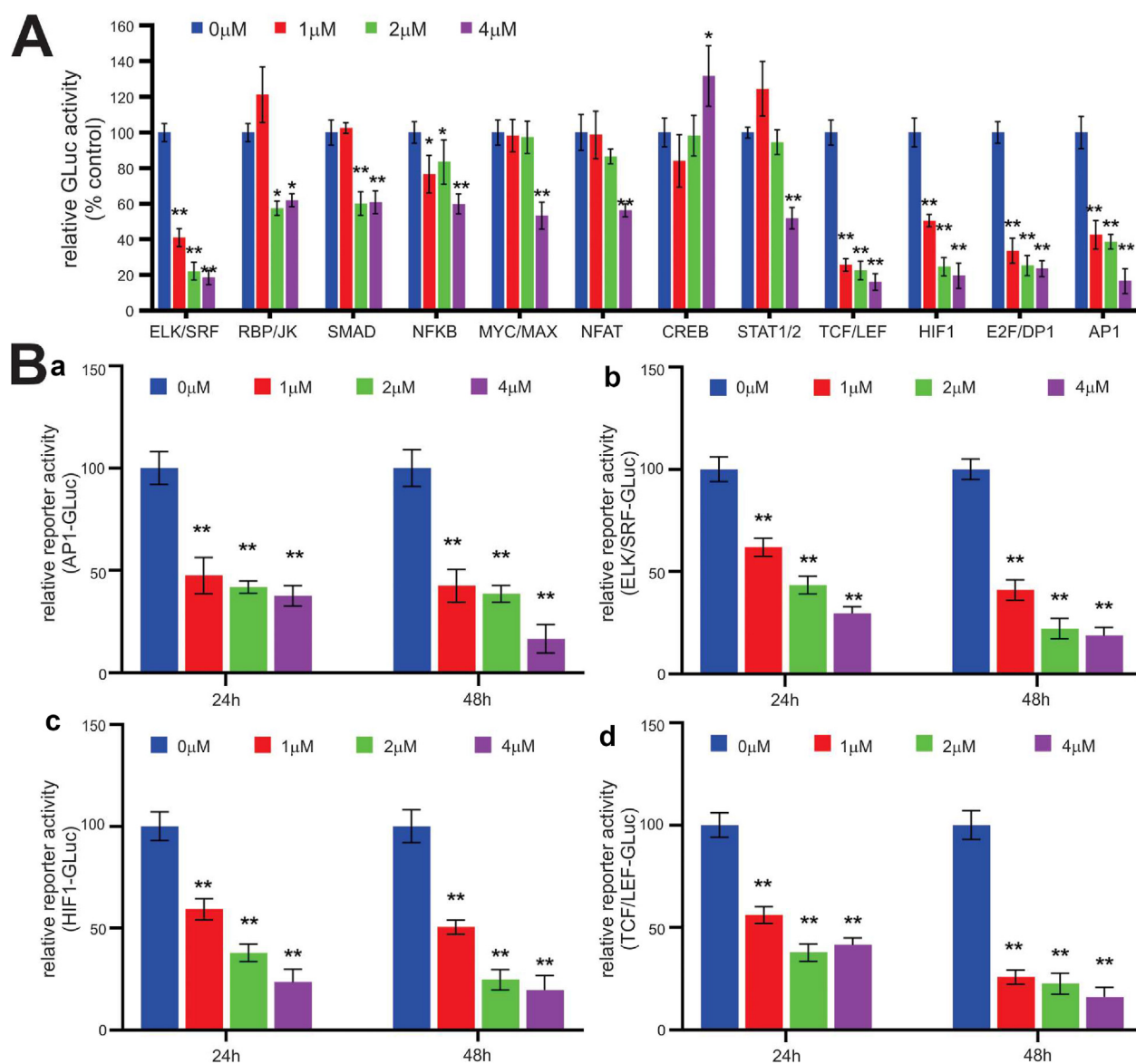


**Figure 5** The inhibitory effects of NA on multiple cancer-associated signaling pathways in human CR ovarian cancer cell lines. **(A)** Effect of NA on the 12 cancer-associated pathways in SKOV3CR cells. SKOV3CR cells were transfected with the Gaussia luciferase reporter plasmids for the 12 cancer-associated pathways and treated with varying concentrations of NA for 48 h. The culture medium was collected for Gaussia luciferase assay using the Gaussia Luciferase Assay Kit (GeneCopoeia, Rockville, MD). Each conditioned assay was done in triplicate. \* $P < 0.05$ , \*\* $P < 0.01$ , compared with that of the cells treated with 0  $\mu$ M NA. **(B)** The inhibitory effect of NA on four cancer-associated pathways in a dose- or time-dependent manner. The four most affected pathway reporter plasmids AP1 (a), ELK/SRF (b), HIF1 (c), and TCF/LEF (d) were transfected into SKOV3CR cells as described in (A). The transfected cells were treated with varying concentrations of NA for 24 h or 48 h. The culture media were taken for Gaussia Luciferase activity assays. Each conditioned assay was done in triplicate. \* $P < 0.05$ , \*\* $P < 0.01$ , compared with that of the cells treated with 0  $\mu$ M NA.

### NA may be repurposed as a novel and efficacious anti-chemoresistant agent for cisplatin-resistant ovarian cancer

While surgical removal of primary tumors followed by platinum-based chemotherapy remains the standard treatment for patients with advanced-stage epithelial ovarian cancer,<sup>3</sup> many patients experience cancer recurrence due to chemotherapeutic resistance to platinum.

Thus, it is imperative to uncover the underlying mechanism of chemoresistance and to identify novel therapeutic agents to overcome such chemoresistance. It is conceivable that the availability of stable chemoresistant ovarian cancer lines will facilitate our efforts to understand and overcome ovarian cancer chemoresistance in order to improve the long-term survival of ovarian cancer patients. Interestingly, several human ovarian cancer lines that are stably and robustly resistant to cisplatin are available in the

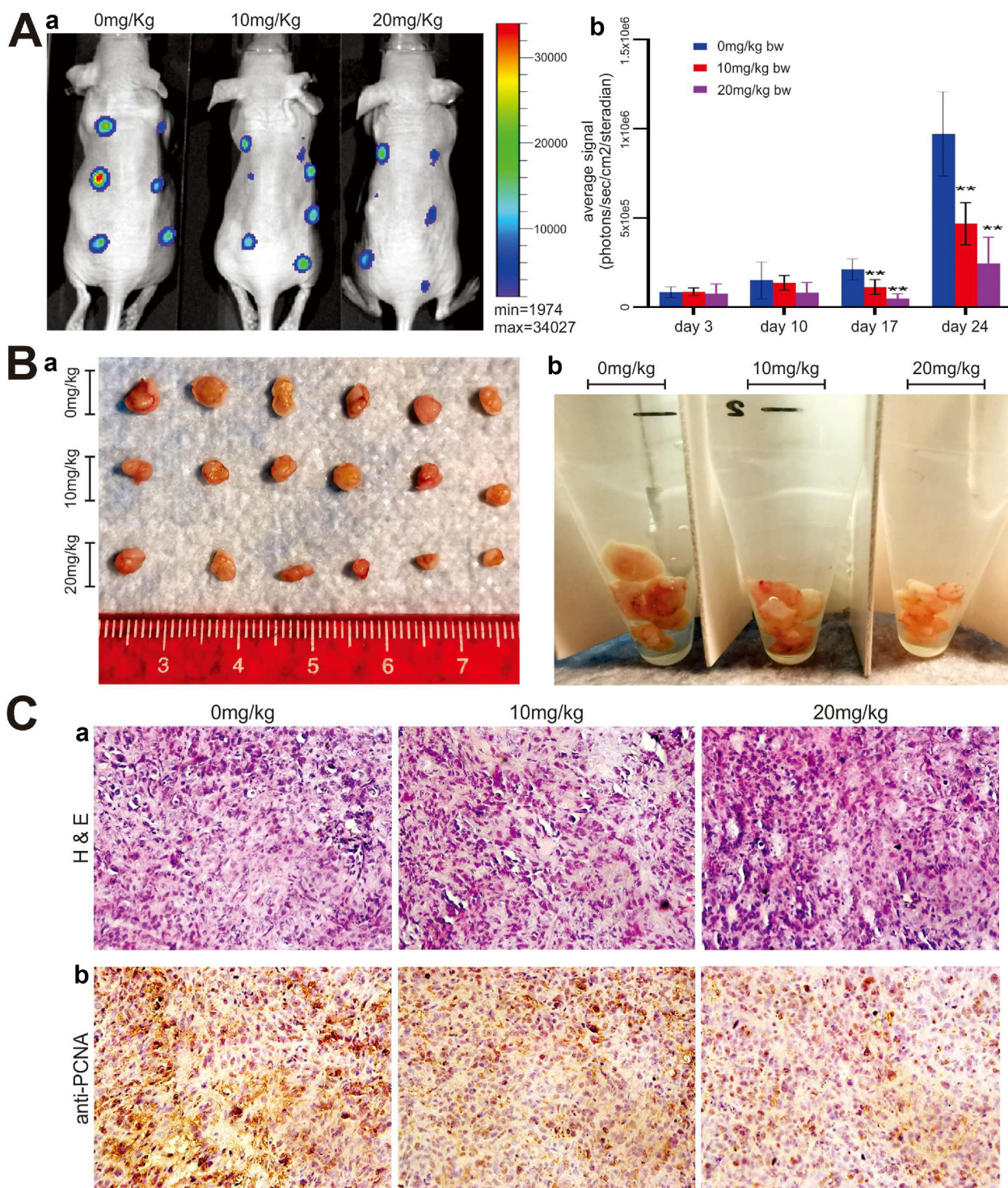


**Figure 6** Suppression of tumor growth by NA in the xenograft tumor model of human CR ovarian cancer cells. **(A)** Firefly luciferase-tagged SKOV3CR cells were injected into the flanks subcutaneously of athymic nude mice ( $n = 6$  per group). At 3 days post-implantation, the mice were randomized into three groups and separately treated with 0, 10, and 20 mg/kg NA for 3 weeks. The mice were imaged at 3, 10, 17, and 24 days after treatment, and sacrificed on day 24. Representative images on day 24 are shown **(a)**. The average signal for each group at different time points was calculated by using Xenogen's Living Image analysis software **(b)**.  $**P < 0.01$ , compared with that of the 0 mg/kg NA group. **(B)** Gross images of retrieved tumor masses. Representative retrieved tumor masses were individually photographed **(a)** or pooled in Eppendorf tubes **(b)**. **(C)** Histologic and IHC analyses. The retrieved tumor masses were subjected to H&E staining **(a)** and anti-PCNA immunohistochemical staining **(b)**. Minus primary antibody and control IgG were used as negative controls. Representative images are shown.

cancer research community,<sup>82,83</sup> although the first cisplatin-resistant ovarian cancer line A2780<sup>CP</sup> or A2780/CP70 was reported in 1988<sup>82–84</sup> and a couple of resistant lines were created from less well-characterized cell lines or treated patients.<sup>85–87</sup> However, most of those lines tolerate relatively low concentrations of cisplatin, and lack of parental vs. resistant lines for comparative mechanism-based studies.

Here, we established the stable cisplatin-resistant lines OVCAR8 and SKOV3 through a cisplatin dose-escalating selection process. We further demonstrated that both lines conferred robust and stable resistance to at least 5  $\mu$ M cisplatin *in vitro*. More importantly, the OVCAR8CR and SKOV3CR lines were shown to share similar biological characteristics to other chemoresistance, especially platinum-resistance cancer lines, and up-regulated the expression of representative chemoresistance-related genes. Therefore, the OVCAR8CR and SKOV3CR lines should be valuable research tools to study cisplatin resistance in ovarian cancer.

Drug repurposing of existing or abandoned drugs represents a cost-effective and time-saving approach to the identification of potentially efficacious therapeutic agents since toxicity and pharmacokinetic profiles are already established for those drugs.<sup>9,10</sup> Anthelmintic drugs are a group of agents to treat intestinal infections caused by parasitic worms (helminths). Niclosamide (NA) is an anthelmintic drug belonging to salicylanilides.<sup>11–14</sup> For the past several years, NA has been shown to exert anti-cancer activity in several malignant tumors including ovarian cancer.<sup>14–32</sup> In this study, our results are the first to demonstrate that NA can overcome cisplatin resistance in human ovarian cancer cells.

Mechanistically, we tested the effect of NA on the 12 cancer-related signaling pathways in the cisplatin-resistant ovarian cancer cells and found that 11 of 12 cancer-related pathways, especially AP1, ELK/SRF, HIF1, and TCF/LEF pathways, were effectively inhibited by NA in a dose-dependent fashion. Our results strongly suggest that NA may exert its anti-chemoresistant activity in cisplatin-resistance human ovarian cancer lines, at least in part, by inhibiting multiple cancer-associated proliferation-related pathways. Consistent with our findings, another study reported that NA effectively inhibited cell proliferation and survival, and angiogenesis of retinoblastoma via targeting Wnt/ $\beta$ -catenin pathway.<sup>88</sup> NA was also shown to inhibit cancer cell stemness, extracellular matrix remodeling, and metastasis by dysregulating the nuclear  $\beta$ -catenin/c-Myc axis in human oral squamous cell carcinoma.<sup>89</sup> In addition, it was reported that NA acted as a potent radiosensitizer via inhibiting STAT3 and Bcl-2 and increasing ROS generation in triple-negative breast cancer (TNBC) cells and xenograft tumors.<sup>90</sup> Thus, while it has been reported that NA can inhibit multiple cellular targets,<sup>13,14,91</sup> it is interesting to investigate whether NA exerts its anti-cancer activity and overcomes chemoresistance through the same or similar mechanisms.

## Conclusions

We sought to investigate whether NA could be repurposed as an effective therapeutic agent to overcome cisplatin resistance in human ovarian cancer cells. To accomplish our

goal, we established two robust CR human ovarian cancer lines that exhibited the essential biological characteristics of cisplatin resistance in human cancer. Using the two CR lines, we demonstrated that NA effectively inhibited cell proliferation, suppressed cell migration, and induced cell apoptosis at a very low micromole range. Furthermore, NA was shown to effectively inhibit xenograft tumor growth of human cisplatin-resistant ovarian cancer cells. Mechanistically, NA was shown to inhibit multiple cancer-related pathways, especially AP1, ELK/SRF, HIF1, and TCF/LEF, in the CR ovarian cancer cells. Taken together, our findings strongly indicate that NA may be repurposed as a novel agent to overcome cisplatin resistance in chemoresistant human ovarian cancer, although further clinical trials are highly warranted.

## Ethics declaration

Since the reported work did not involve the use of clinical samples and/or human subject enrollment, no approval from the Institutional Review Board (IRB) was required. However, we obtained approvals from the Institutional Biosafety Committee (IBC) and the Institutional Committee of Animal Use and Care (IACUC) prior to commencing this study, since the reported work needed to be performed under biosafety level 2 (BSL2) and involved in the use of athymic nude mice.

## Author contributions

TCH, LZ, LH, and LS were responsible for the conception and design of the study. LH, LZ, JZ, YD, HW, and PZ performed the experiments and were involved in the collection, analysis, and interpretation of the data. GZ, WZ, YW, WW, and CC provided technical assistance and/or experimental resources that were essential to the study. LH, LZ, RRR, RCH, HHL, LS, and TCH drafted the manuscript. All authors read and edited the draft manuscript, and approved the final version of the manuscript.

## Conflict of interests

The authors declare no competing conflict of interests.

## Funding

The reported work was supported in part by research grants from the National Institutes of Health (No. CA226303 to TCH, and No. DE030480 to RRR). WW was supported by the Medical Scientist Training Program of the National Institutes of Health (USA) (No. T32 GM007281). This project was also supported in part by The University of Chicago Cancer Center Support Grant (No. P30CA014599) and the National Center for Advancing Translational Sciences of the National Institutes of Health (USA) (No. UL1 TR000430). TCH was also supported by the Mabel Green Myers Research Endowment Fund and The University of Chicago Orthopaedics Alumni Fund. Funding sources were not involved in the study design, collection, analysis & interpretation of data,

writing of the report, and the decision to submit the paper for publication.

## Data availability statement

The data that supports the findings of this study are available in the supplementary material of this article or on request from the corresponding authors.

## Acknowledgements

The authors wish to thank Dr. Ernest Lengyel of The University of Chicago for providing the human ovarian cancer cell lines OVCAR8, SKOV3, OVPA8, and OVCAR3.

## Appendix A. Supplementary data

Supplementary data to this article can be found online at <https://doi.org/10.1016/j.gendis.2022.12.005>.

## References

- Siegel RL, Miller KD, Fuchs HE, et al. Cancer statistics, 2021. *CA Cancer J Clin.* 2021;71(1):7–33.
- Matulonis UA, Sood AK, Fallowfield L, et al. Ovarian cancer. *Nat Rev Dis Primers.* 2016;2:16061.
- Lheureux S, Braunstein M, Oza AM. Epithelial ovarian cancer: evolution of management in the era of precision medicine. *CA Cancer J Clin.* 2019;69(4):280–304.
- Reid BM, Permuth JB, Sellers TA. Epidemiology of ovarian cancer: a review. *Cancer Biol Med.* 2017;14(1):9–32.
- Lynch HT, Casey MJ, Snyder CL, et al. Hereditary ovarian carcinoma: heterogeneity, molecular genetics, pathology, and management. *Mol Oncol.* 2009;3(2):97–137.
- Goode EL, Chenevix-Trench G, Song H, et al. A genome-wide association study identifies susceptibility loci for ovarian cancer at 2q31 and 8q24. *Nat Genet.* 2010;42(10):874–879.
- Kuroki L, Guntupalli SR. Treatment of epithelial ovarian cancer. *BMJ.* 2020;371:m3773.
- Kurnit KC, Fleming GF, Lengyel E. Updates and new options in advanced epithelial ovarian cancer treatment. *Obstet Gynecol.* 2021;137(1):108–121.
- Pushpakom S, Iorio F, Eyers PA, et al. Drug repurposing: progress, challenges and recommendations. *Nat Rev Drug Discov.* 2019;18(1):41–58.
- Scholnik-Cabrera A, Juárez-López D, Duenas-Gonzalez A. Perspectives on drug repurposing. *Curr Med Chem.* 2021;28(11):2085–2099.
- Sleire L, Førde HE, Netland IA, et al. Drug repurposing in cancer. *Pharmacol Res.* 2017;124:74–91.
- Tran AA, Prasad V. Drug repurposing for cancer treatments: a well-intentioned, but misguided strategy. *Lancet Oncol.* 2020;21(9):1134–1136.
- Pantziarka P, Vandeborne L, Bouche G. A database of drug repurposing clinical trials in oncology. *Front Pharmacol.* 2021;12:790952.
- Barbosa EJ, Löbenberg R, de Araujo GLB, et al. Niclosamide repositioning for treating cancer: challenges and nano-based drug delivery opportunities. *Eur J Pharm Biopharm.* 2019;141:58–69.
- Jin Y, Lu Z, Ding K, et al. Antineoplastic mechanisms of niclosamide in acute myelogenous leukemia stem cells: inactivation of the NF-kappaB pathway and generation of reactive oxygen species. *Cancer Res.* 2010;70(6):2516–2527.
- Osada T, Chen M, Yang XY, et al. Anthelmintic compound niclosamide downregulates Wnt signaling and elicits antitumor responses in tumors with activating APC mutations. *Cancer Res.* 2011;71(12):4172–4182.
- Lu W, Lin C, Roberts MJ, et al. Niclosamide suppresses cancer cell growth by inducing Wnt co-receptor LRP6 degradation and inhibiting the Wnt/ $\beta$ -catenin pathway. *PLoS One.* 2011;6(12):e29290.
- Sack U, Walther W, Scudiero D, et al. Novel effect of anti-helminthic Niclosamide on S100A4-mediated metastatic progression in colon cancer. *J Natl Cancer Inst.* 2011;103(13):1018–1036.
- Yo YT, Lin YW, Wang YC, et al. Growth inhibition of ovarian tumor-initiating cells by niclosamide. *Mol Cancer Therapeut.* 2012;11(8):1703–1712.
- Li R, Hu Z, Sun SY, et al. Niclosamide overcomes acquired resistance to erlotinib through suppression of STAT3 in non-small cell lung cancer. *Mol Cancer Therapeut.* 2013;12(10):2200–2212.
- Wieland A, Trageser D, Gogolok S, et al. Anticancer effects of niclosamide in human glioblastoma. *Clin Cancer Res.* 2013;19(15):4124–4136.
- You S, Li R, Park D, et al. Disruption of STAT3 by niclosamide reverses radioresistance of human lung cancer. *Mol Cancer Therapeut.* 2014;13(3):606–616.
- Londoño-Joshi AI, Arend RC, Aristizabal L, et al. Effect of niclosamide on basal-like breast cancers. *Mol Cancer Therapeut.* 2014;13(4):800–811.
- Arend RC, Londoño-Joshi AI, Samant RS, et al. Inhibition of Wnt/ $\beta$ -catenin pathway by niclosamide: a therapeutic target for ovarian cancer. *Gynecol Oncol.* 2014;134(1):112–120.
- Liu C, Lou W, Zhu Y, et al. Niclosamide inhibits androgen receptor variants expression and overcomes enzalutamide resistance in castration-resistant prostate cancer. *Clin Cancer Res.* 2014;20(12):3198–3210.
- King ML, Lindberg ME, Stodden GR, et al. WNT7A/ $\beta$ -catenin signaling induces FGF<sub>1</sub> and influences sensitivity to niclosamide in ovarian cancer. *Oncogene.* 2015;34(26):3452–3462.
- Liao Z, Nan G, Yan Z, et al. The anthelmintic drug niclosamide inhibits the proliferative activity of human osteosarcoma cells by targeting multiple signal pathways. *Curr Cancer Drug Targets.* 2015;15(8):726–738.
- Chen B, Wei W, Ma L, et al. Computational discovery of niclosamide ethanolamine, a repurposed drug candidate that reduces growth of hepatocellular carcinoma cells *in vitro* and in mice by inhibiting cell division cycle 37 signaling. *Gastroenterology.* 2017;152(8):2022–2036.
- Yu X, Liu F, Zeng L, et al. Niclosamide exhibits potent anticancer activity and synergizes with sorafenib in human renal cell cancer cells. *Cell Physiol Biochem.* 2018;47(3):957–971.
- Schweizer MT, Haugk K, McKiernan JS, et al. A phase I study of niclosamide in combination with enzalutamide in men with castration-resistant prostate cancer. *PLoS One.* 2018;13(6):e0198389.
- Burock S, Daum S, Keilholz U, et al. Phase II trial to investigate the safety and efficacy of orally applied niclosamide in patients with metachronous or synchronous metastases of a colorectal cancer progressing after therapy: the NIKOLO trial. *BMC Cancer.* 2018;18:297.
- Deng Y, Wang Z, Zhang F, et al. A blockade of IGF signaling sensitizes human ovarian cancer cells to the anthelmintic niclosamide-induced anti-proliferative and anticancer activities. *Cell Physiol Biochem.* 2016;39(3):871–888.
- Mao Y, Ni N, Huang L, et al. Argonaute (AGO) proteins play an essential role in mediating BMP9-induced osteogenic signaling

- in mesenchymal stem cells (MSCs). *Genes Dis.* 2021;8(6):918–930.
34. Ni N, Deng F, He F, et al. A one-step construction of adenovirus (OSCA) system using the Gibson DNA Assembly technology. *Mol Ther Oncolytics.* 2021;23:602–611.
  35. Wu X, Li Z, Zhang H, et al. Modeling colorectal tumorigenesis using the organoids derived from conditionally immortalized mouse intestinal crypt cells (ciMICs). *Genes Dis.* 2021;8(6):814–826.
  36. Huang L, Zhao L, Zhang J, et al. Antiparasitic mebendazole (MBZ) effectively overcomes cisplatin resistance in human ovarian cancer cells by inhibiting multiple cancer-associated signaling pathways. *Aging.* 2021;13(13):17407–17427.
  37. Cui J, Gong M, Fang S, et al. All-trans retinoic acid reverses malignant biological behavior of hepatocarcinoma cells by regulating miR-200 family members. *Genes Dis.* 2021;8(4):509–520.
  38. Luther GA, Lamplot J, Chen X, et al. IGFBP5 domains exert distinct inhibitory effects on the tumorigenicity and metastasis of human osteosarcoma. *Cancer Lett.* 2013;336(1):222–230.
  39. Su Y, Wagner ER, Luo Q, et al. Insulin-like growth factor binding protein 5 suppresses tumor growth and metastasis of human osteosarcoma. *Oncogene.* 2011;30(37):3907–3917.
  40. Deng Y, Zhang J, Wang Z, et al. Antibiotic monensin synergizes with EGFR inhibitors and oxaliplatin to suppress the proliferation of human ovarian cancer cells. *Sci Rep.* 2015;5:17523.
  41. Yu X, Chen L, Wu K, et al. Establishment and functional characterization of the reversibly immortalized mouse glomerular podocytes (imPODs). *Genes Dis.* 2018;5(2):137–149.
  42. Shu Y, Wu K, Zeng Z, et al. A simplified system to express circularized inhibitors of miRNA for stable and potent suppression of miRNA functions. *Mol Ther Nucleic Acids.* 2018;13:556–567.
  43. Shu Y, Yang C, Ji X, et al. Reversibly immortalized human umbilical cord-derived mesenchymal stem cells (UC-MSCs) are responsive to BMP9-induced osteogenic and adipogenic differentiation. *J Cell Biochem.* 2018;119(11):8872–8886.
  44. Luo Q, Kang Q, Si W, et al. Connective tissue growth factor (CTGF) is regulated by Wnt and bone morphogenetic proteins signaling in osteoblast differentiation of mesenchymal stem cells. *J Biol Chem.* 2004;279(53):55958–55968.
  45. Huang B, Huang LF, Zhao L, et al. Microvesicles (MIVs) secreted from adipose-derived stem cells (ADSCs) contain multiple microRNAs and promote the migration and invasion of endothelial cells. *Genes Dis.* 2020;7(2):225–234.
  46. Si W, Kang Q, Luu HH, et al. CCN1/Cyr61 is regulated by the canonical Wnt signal and plays an important role in Wnt3A-induced osteoblast differentiation of mesenchymal stem cells. *Mol Cell Biol.* 2006;26(8):2955–2964.
  47. Zhou L, An N, Haydon RC, et al. Tyrosine kinase inhibitor STI-571/gleevec down-regulates the  $\beta$ -catenin signaling activity. *Cancer Lett.* 2003;193(2):161–170.
  48. Shu Y, Wang Y, Lv WQ, et al. ARRB1-promoted NOTCH1 degradation is suppressed by OncomiR miR-223 in T-cell acute lymphoblastic leukemia. *Cancer Res.* 2020;80(5):988–998.
  49. Zhang Q, Wang J, Deng F, et al. TqPCR: a touchdown qPCR assay with significantly improved detection sensitivity and amplification efficiency of SYBR green qPCR. *PLoS One.* 2015;10(7):e0132666.
  50. Fan J, Wei Q, Liao J, et al. Noncanonical Wnt signaling plays an important role in modulating canonical Wnt-regulated stemness, proliferation and terminal differentiation of hepatic progenitors. *Oncotarget.* 2017;8(16):27105–27119.
  51. Liu W, Deng Z, Zeng Z, et al. Highly expressed BMP9/GDF2 in postnatal mouse liver and lungs may account for its pleiotropic effects on stem cell differentiation, angiogenesis, tumor growth and metabolism. *Genes Dis.* 2020;7(2):235–244.
  52. He F, Ni N, Wang H, et al. OUHP: an optimized universal hairpin primer system for cost-effective and high-throughput RT-qPCR-based quantification of microRNA (miRNA) expression. *Nucleic Acids Res.* 2022;50(4):e22.
  53. Zeng Z, Huang B, Wang X, et al. A reverse transcriptase-mediated ribosomal RNA depletion (RTR2D) strategy for the cost-effective construction of RNA sequencing libraries. *J Adv Res.* 2020;24:239–250.
  54. Gao JL, Lv GY, He BC, et al. Ginseng saponin metabolite 20(S)-protopanaxadiol inhibits tumor growth by targeting multiple cancer signaling pathways. *Oncol Rep.* 2013;30(1):292–298.
  55. He BC, Gao JL, Zhang BQ, et al. Tetrandrine inhibits Wnt/ $\beta$ -catenin signaling and suppresses tumor growth of human colorectal cancer. *Mol Pharmacol.* 2011;79(2):211–219.
  56. Wang X, Zhao L, Wu X, et al. Development of a simplified and inexpensive RNA depletion method for plasmid DNA purification using size selection magnetic beads (SSMBs). *Genes Dis.* 2021;8(3):298–306.
  57. Fan J, Feng Y, Zhang R, et al. A simplified system for the effective expression and delivery of functional mature microRNAs in mammalian cells. *Cancer Gene Ther.* 2020;27(6):424–437.
  58. Liao J, Wei Q, Fan J, et al. Characterization of retroviral infectivity and superinfection resistance during retrovirus-mediated transduction of mammalian cells. *Gene Ther.* 2017;24(6):333–341.
  59. Luo J, Tang M, Huang J, et al. TGF $\beta$ /BMP type I receptors ALK1 and ALK2 are essential for BMP9-induced osteogenic signaling in mesenchymal stem cells. *J Biol Chem.* 2010;285(38):29588–29598.
  60. Zeng Z, Huang B, Huang S, et al. The development of a sensitive fluorescent protein-based transcript reporter for high throughput screening of negative modulators of lncRNAs. *Genes Dis.* 2018;5(1):62–74.
  61. Zhao C, Qazvini NT, Sadati M, et al. A pH-triggered, self-assembled, and bioprintable hybrid hydrogel scaffold for mesenchymal stem cell based bone tissue engineering. *ACS Appl Mater Interfaces.* 2019;11(9):8749–8762.
  62. Zou Y, Qazvini NT, Zane K, et al. Gelatin-derived graphene-silicate hybrid materials are biocompatible and synergistically promote BMP9-induced osteogenic differentiation of mesenchymal stem cells. *ACS Appl Mater Interfaces.* 2017;9(19):15922–15932.
  63. Luo X, Chen J, Song WX, et al. Osteogenic BMPs promote tumor growth of human osteosarcomas that harbor differentiation defects. *Lab Invest.* 2008;88(12):1264–1277.
  64. Zhao X, Huang B, Wang H, et al. A functional autophagy pathway is essential for BMP9-induced osteogenic differentiation of mesenchymal stem cells (MSCs). *Am J Transl Res.* 2021;13(5):4233–4250.
  65. Huang E, Zhu G, Jiang W, et al. Growth hormone synergizes with BMP9 in osteogenic differentiation by activating the JAK/STAT/IGF1 pathway in murine multilineage cells. *J Bone Miner Res.* 2012;27(7):1566–1575.
  66. Wang X, Wu X, Zhang Z, et al. Monensin inhibits cell proliferation and tumor growth of chemo-resistant pancreatic cancer cells by targeting the EGFR signaling pathway. *Sci Rep.* 2018;8:17914.
  67. Zhao L, Huang L, Zhang J, et al. The inhibition of BRAF activity sensitizes chemoresistant human ovarian cancer cells to paclitaxel-induced cytotoxicity and tumor growth inhibition. *Am J Transl Res.* 2020;12(12):8084–8098.
  68. Gou Y, Weng Y, Chen Q, et al. Carboxymethyl chitosan prolongs adenovirus-mediated expression of IL-10 and ameliorates hepatic fibrosis in a mouse model. *Bioeng Transl Med.* 2022;7(3):e10306.
  69. Hu X, Li L, Yu X, et al. CRISPR/Cas9-mediated reversibly immortalized mouse bone marrow stromal stem cells (BMSCs)

- retain multipotent features of mesenchymal stem cells (MSCs). *Oncotarget*. 2017;8(67):111847–111865.
70. He F, Ni N, Zeng Z, et al. FAMSis: a synthetic biology approach to the fast assembly of multiplex siRNAs for silencing gene expression in mammalian cells. *Mol Ther Nucleic Acids*. 2020;22:885–899.
  71. Wang X, Yuan C, Huang B, et al. Developing a versatile shotgun cloning strategy for single-vector-based multiplex expression of short interfering RNAs (siRNAs) in mammalian cells. *ACS Synth Biol*. 2019;8(9):2092–2105.
  72. Zhang B, Yang L, Zeng Z, et al. Leptin potentiates BMP9-induced osteogenic differentiation of mesenchymal stem cells through the activation of JAK/STAT signaling. *Stem Cell Dev*. 2020;29(8):498–510.
  73. Cao D, Lei Y, Ye Z, et al. Blockade of IGF/IGF-1R signaling axis with soluble IGF-1R mutants suppresses the cell proliferation and tumor growth of human osteosarcoma. *Am J Cancer Res*. 2020;10(10):3248–3266.
  74. An L, Shi Q, Zhu Y, et al. Bone morphogenetic protein 4 (BMP4) promotes hepatic glycogen accumulation and reduces glucose level in hepatocytes through mTORC2 signaling pathway. *Genes Dis*. 2021;8(4):531–544.
  75. Zhong J, Kang Q, Cao Y, et al. BMP4 augments the survival of hepatocellular carcinoma (HCC) cells under hypoxia and hypoglycemia conditions by promoting the glycolysis pathway. *Am J Cancer Res*. 2021;11(3):793–811.
  76. Zhong J, Wang H, Yang K, et al. Reversibly immortalized keratinocytes (iKera) facilitate re-epithelization and skin wound healing: potential applications in cell-based skin tissue engineering. *Bioact Mater*. 2022;9:523–540.
  77. Liu Q, Wang Z, Jiang Y, et al. Single-cell landscape analysis reveals distinct regression trajectories and novel prognostic biomarkers in primary neuroblastoma. *Genes Dis*. 2022;9(6):1624–1638.
  78. Zhang P, Zhang Z, Zhou X, et al. Identification of genes associated with cisplatin resistance in human oral squamous cell carcinoma cell line. *BMC Cancer*. 2006;6:224.
  79. Shen DW, Pouliot LM, Hall MD, et al. Cisplatin resistance: a cellular self-defense mechanism resulting from multiple epigenetic and genetic changes. *Pharmacol Rev*. 2012;64(3):706–721.
  80. Amable L. Cisplatin resistance and opportunities for precision medicine. *Pharmacol Res*. 2016;106:27–36.
  81. Makovec T. Cisplatin and beyond: molecular mechanisms of action and drug resistance development in cancer chemotherapy. *Radiol Oncol*. 2019;53(2):148–158.
  82. Parker RJ, Eastman A, Bostick-Bruton F, et al. Acquired cisplatin resistance in human ovarian cancer cells is associated with enhanced repair of cisplatin-DNA lesions and reduced drug accumulation. *J Clin Invest*. 1991;87(3):772–777.
  83. Zhen W, Link Jr CJ, O'Connor PM, et al. Increased gene-specific repair of cisplatin interstrand cross-links in cisplatin-resistant human ovarian cancer cell lines. *Mol Cell Biol*. 1992;12(9):3689–3698.
  84. Lai GM, Ozols RF, Smyth JF, et al. Enhanced DNA repair and resistance to cisplatin in human ovarian cancer. *Biochem Pharmacol*. 1988;37(24):4597–4600.
  85. Yao KS, Godwin AK, Johnson SW, et al. Evidence for altered regulation of gamma-glutamylcysteine synthetase gene expression among cisplatin-sensitive and cisplatin-resistant human ovarian cancer cell lines. *Cancer Res*. 1995;55(19):4367–4374.
  86. Perego P, Romanelli S, Carenini N, et al. Ovarian cancer cisplatin-resistant cell lines: multiple changes including collateral sensitivity to Taxol. *Ann Oncol*. 1998;9(4):423–430.
  87. Judson PL, Watson JM, Gehrig PA, et al. Cisplatin inhibits paclitaxel-induced apoptosis in cisplatin-resistant ovarian cancer cell lines: possible explanation for failure of combination therapy. *Cancer Res*. 1999;59(10):2425–2432.
  88. Li Z, Li Q, Wang G, et al. Inhibition of Wnt/ $\beta$ -catenin by anthelmintic drug niclosamide effectively targets growth, survival, and angiogenesis of retinoblastoma. *Am J Transl Res*. 2017;9(8):3776–3786.
  89. Wang LH, Xu M, Fu LQ, et al. The antihelminthic niclosamide inhibits cancer stemness, extracellular matrix remodeling, and metastasis through dysregulation of the nuclear  $\beta$ -catenin/c-myc axis in OSCC. *Sci Rep*. 2018;8:12776.
  90. Lu L, Dong J, Wang L, et al. Activation of STAT3 and Bcl-2 and reduction of reactive oxygen species (ROS) promote radioresistance in breast cancer and overcome of radioresistance with niclosamide. *Oncogene*. 2018;37(39):5292–5304.
  91. Li Y, Li PK, Roberts MJ, et al. Multi-targeted therapy of cancer by niclosamide: a new application for an old drug. *Cancer Lett*. 2014;349(1):8–14.